

ORIGINAL ARTICLE

FcRn binding is not sufficient for achieving systemic therapeutic levels of immunoglobulin G after oral delivery of enteric-coated capsules in cynomolgus macaques

Salman Muzammil¹, John R. Mabus¹, Philip R. Cooper¹, Randall J. Brezski¹, Courtney B. Bement¹, Rob Perkinson¹, Norman D. Huebert², Suzanne Thompson³, Dalia Levine¹, Connie Kliwinski¹, Dino Bradley² & Pamela J. Hornby¹

¹Janssen Biopharmaceuticals (formerly Biotechnology Center of Excellence), R&D of J&J, Spring House, Pennsylvania 19477

²Discovery Sciences, Janssen Pharmaceutical R&D of J&J, Spring House, Pennsylvania 19477

³Preclinical Center of Excellence Ethicon, Inc., Cincinnati, Ohio 45242

Keywords

Immunoglobulin G, epithelial cell, transcytosis, Fc receptor, oral bioavailability, translational, cynomolgus macaques

Correspondence

Pamela J. Hornby, Janssen Pharmaceutical R&D, Cardiovascular & Metabolic Disease, SH42-2510-A, 1440 McKean Road, Spring House, PA 19477.

Tel: 215 628 7187; Fax: 215 540 4621;

E-mail: phornby@its.jnj.com

Funding Information

No funding information provided.

Received: 30 October 2015; Revised: 22 December 2015; Accepted: 14 January 2016

Pharma Res Per, 4(3), 2016, e00218, doi: 10.1002/prp2.218

doi: 10.1002/prp2.218

Abstract

Although much speculation has surrounded intestinally expressed FcRn as a means for systemic uptake of orally administered immunoglobulin G (IgG), this has not been validated in translational models beyond neonates or in FcRn-expressing cells in vitro. Recently, IgG1 intestinal infusion acutely in anesthetized cynomolgus resulted in detectable serum monoclonal antibody (mAb) levels. In this study, we show that IgG2 has greater protease resistance to intestinal enzymes in vitro and mice in vivo, due to protease resistance in the hinge region. An IgG2 mAb engineered for FcRn binding, was optimally formulated, lyophilized, and loaded into enteric-coated capsules for oral dosing in cynomolgus. Small intestinal pH 7.5 was selected for enteric delivery based on gastrointestinal pH profiling of cynomolgus by operator-assisted IntelliCap System[®]. Milling of the lyophilized IgG2 M428L FcRn-binding variant after formulation in 10 mmol/L histidine, pH 5.7, 8.5% sucrose, 0.04% PS80 did not alter the physicochemical properties nor the molecular integrity compared to the batch released in PBS. Size 3 hard gel capsules (23.2 mg IgG2 M428L ~3 mg/kg) were coated with hydroxypropyl methylcellulose acetate succinate for rapid dissolution at pH 7.5 in small intestine and FcRn binding of encapsulated mAb confirmed. Initial capsule dosing by endoscopic delivery into the small intestine achieved 0.2 + 0.1 ng/mL ($n = 5$) peak at 24 h. Weekly oral capsule dosing for 6 weeks achieved levels of 0.4 + 0.2 ng/mL and, despite increasing the dose and frequency, remained below 1 ng/mL. In conclusion, lyophilized milled mAb retains FcRn binding and molecular integrity for small intestinal delivery. The low systemic exposure has demonstrated the limitations of intestinal FcRn in non-human primates and the unfeasibility of employing this for therapeutic levels of mAb. Local mAb delivery with limited systemic exposure may be sufficient as a therapeutic for intestinal diseases.

Abbreviations

DF, diafiltration; DLS, dynamic light scattering; DPBS, Dulbecco's phosphate buffered saline; DSC, differential scanning calorimetry; FaSSIF, fasting Simulated Small Intestinal Fluid; FB, formulated bulk; HPC, hydroxyl propyl cellulose; HPMCAS, hydroxypropyl methylcellulose acetate succinate; MSD, mesoscale discovery; PEG, polyethylene glycol; RLU, relative luminescent units; RSV, antirespiratory syncytial virus; UF, ultrafiltration; WT, wild-type.

Introduction

Monoclonal antibodies (mAb) are not orally administered therapeutically due to their degradation by digestive enzymes in the gastrointestinal tract and by low intestinal permeation. Permeation of proteins through the intestinal wall is typically limited to peptides of four amino acids or less (or molecules <800 Da) due to the presence of tight junctions between epithelial cells that, combined with mAb polarity, makes them unlikely to be absorbed in normal intestine. In neonates, immunoglobulins (Ig) from suckled milk are transported across intestinal epithelial cells via the neonatal Fc receptor (FcRn; also Brambell receptor) and this active transport system achieves high (~30%) fractional uptake of orally or intestinally delivered mAbs (Martin *et al.* 1997; Kliwinski *et al.* 2013). The idea that FcRn in the intestine could be targeted as a means for obtaining therapeutic levels of IgG or Fc fusion proteins subsequent to their oral delivery is almost as old as the finding that it retains expression in intestines of adult primate (Israel *et al.* 1997). Oral delivery continues to be invoked as a biotechnical possibility (Bitonti *et al.* 2004; Low *et al.* 2005; Blumberg *et al.* 2009; Pridgen *et al.* 2013), but has not been validated to date in a translational model. In contrast, pulmonary delivery of Fc fusion protein or mAb via bronchiole epithelial cell FcRn has been validated in cynomolgus monkey for therapeutically relevant serum levels (Bitonti *et al.* 2004; Low *et al.* 2005).

In intestinal cells, a combination of endocytosis (Mohanty *et al.* 2013) and surface FcRn binding to IgG at pH 6 (Cooper *et al.* 2014) results in FcRn-bound IgG within endosomes (He *et al.* 2008) and transytosis (Claypool *et al.* 2004). The circulating half-life of IgG depends on FcRn binding on endothelial cells (Petkova *et al.* 2006; Kuo and Aveson 2011) and Fc mutations by amino acid replacements of residues in the CH2-3 region to increase FcRn binding affinity, which enhances circulating serum half-life (Suzuki *et al.* 2010; Kuo and Aveson 2011). Using similar FcRn binding affinity mutations also corresponded to their uptake by intestinal FcRn in neonatal rat pups (Kliwinski *et al.* 2013; Cooper *et al.* 2014). However, high-FcRn binding at pH 6.0 was associated with increased affinity at pH 7.4 and resulted in lower systemic mAb levels (Cooper *et al.* 2014), suggesting that moderate FcRn binding affinity at pH 6.0 with no binding at pH 7.4 is preferable for enterocyte transcytosis.

After weaning, FcRn expression in the intestine decreases dramatically and is functionally irrelevant in rodents (Benlounes *et al.* 1995; Kliwinski *et al.* 2013). This limits the utility of using rodents to study FcRn intestinal uptake of IgG, although FcRn-mediated uptake of nanoparticles has been reported in mice (Pridgen *et al.* 2013) and human FcRn transgenic mice are available. In

contrast, expression of FcRn is maintained in the adult human and non-human primate intestine (Israel *et al.* 1997; Hornby *et al.* 2014) with the highest relative FcRn expression in the proximal colon of adult human intestine (Hornby *et al.* 2014). Since it is not clear to what extent results obtained in rodents, based on either rodent or transgenic human FcRn are translational to human, we have performed studies in cynomolgus macaques to address the functional significance. Wild-type mAb and variants with differing FcRn binding affinities delivered acutely into the intestine resulted in detectable circulating levels of full-length mAb, whereas oral delivery resulted in undetectable serum mAb levels (Hornby *et al.* 2014). Although that acute study was limited by the small number of cynomolgus used and variability in the results, greater serum levels of mAb were detected after distal small intestine/proximal colon administration, than following upper intestinal dosing. The individual variability in cynomolgus could not be ascribed to gene variants encoding FcRn, since amino acid residues expected to affect FcRn functionality were not found in this species (Uno *et al.* 2014). Aside from the variability, another concern was that the fractional uptake of full-length FcRn-binding mAb (~0.3%) was relatively low at the terminal timepoint of 90 min. We rationalized that engineering an intestinal protease-resistant mAb with moderately high-FcRn binding affinity could improve on this level of uptake with the potential for a longer half-life to increase systemic exposure upon repeat administration.

In this study, we engineered a mAb (IgG2) with increased resistance to intestinal proteases and FcRn binding affinity. Here, we describe (1) the determination of its stability in intestinal fluid and FcRn binding, (2) the cynomolgus GI pH profile using IntelliCap System[®] (Medimetrics, Briarcliff Manor, New York) operator-assisted monitoring, (3) retention of the mAb FcRn binding and biophysical properties after formulation optimization, lyophilization, and encapsulation, and (4) detectable but low systemic levels of mAb following single and repeated dosing up to 10 weeks in 6 monkeys.

These results did not validate FcRn as a sufficient mechanism for intestinal mAb uptake in order to warrant pursuing this as a biotherapeutic oral delivery strategy. However, engineering intestinal protease resistance may enable local mAb delivery to therapeutic targets in the intestine to improve efficacy and convenience by using enteric-coated protease resistance mAb. Local intestinal delivery by *Lactococcus lactis* that were engineered to secrete IL-10 (Steidler *et al.* 2000; Vandenbroucke *et al.* 2010) and orally delivered bovine polyclonal anti-TNF (Bhol *et al.* 2013) were beneficial in preclinical models.

These data were presented in abstract form (Mabus *et al.* 2014).

Materials and Methods

All animal studies were performed in accordance with the Federal Animal Welfare Act and protocols were approved by the Institutional Animal Care and Use Committee at Janssen Pharmaceutical R&D, Biotechnology Center of Excellence.

In vivo studies

IntelliCap[®] intestinal profiling and dosing

Intestinal pH in cynomolgus has not been previously reported. Intestinal pH profiling and dosing was performed by IntelliCap System[®] capsules (~size 000 containing ~184 μ L), which are approved for clinical use for profiling (Maurer et al. 2015) and drug delivery (Becker et al. 2014) by operator-controlled computer monitoring. Nine monkeys (six fasted o/n and three fed) were given empty IntelliCap System[®] capsules (~size 000) by oral dosing for profiling gastrointestinal pH. For the intestinal transit profiling arm, the IntelliCap drug reservoir was filled with water and finished with mineral oil (Drakeol[®] 600 MIN OIL USP by Calumet, specific gravity 0.8674, viscosity 103.94 cST at 40°C) in the spiral channel. Capsules were dosed orally to monkeys ($n = 9$) under fasted ($n = 6$) or fed ($n = 3$) conditions and monitoring continued until the monkey voided the capsule or the end of the signaling life of the capsule.

Six beagle dogs (range 9.1–12.4 kg) were orally dosed with IntelliCap[™] capsules (~size 000) which were filled with mAb for a final fixed dose of ~ 3 mg/kg. For the intestinal dosing in beagle dogs, the IntelliCap System[®] drug reservoir was filled with the test article and finished with mineral oil as described. Capsules were prepared and loaded manually with mAb not more than 24 h prior to administration.

Enteric-coated capsule dosing

Video gastroendoscopy was used for single dosing of monkeys with enteric-coated (size 3) capsules. The correct location was reached using a specially designed snare. Each hard gelatin enteric-coated capsule contained 54 mg of drug product, of which 18 mg was hIgG2 M428L. The highest endotoxin level in the mAb dosed was 1.0 EU/kg. Capsules were coated with hydroxypropyl methylcellulose acetate succinate (HPMCAS) to ensure that coating dissolution and mAb release occurred within 20 min of exposure to pH 7.5, which is the pH in the midsmall intestine (jejunoileum).

A total of six monkeys (6 female; weight 3.4–3.85 kg) were dosed with enteric-coated capsules according to the

following procedures: For capsule dosing initially, gastroendoscopy was used to deliver the capsules close to where dissolution was expected to occur in the small intestine and avoided the risk of delayed gastric emptying of the capsule. Single capsule oral delivery was performed under isoflurane anesthesia using a flexible pediatric endoscope, as reported previously (Hornby et al. 2014). Briefly, anesthetized animals were placed in dorsal or lateral recumbent position and the endoscope (Olympus GIF-XP160 Video Gastroscope with 5.9 mm diameter, 2.0 mm channel, 103 cm working length) with a 12 mm diameter, 8–12 inch flexible overtube (to maintain a pathway through the pharynx) was passed through the mouth, esophagus, and stomach where the pylorus was identified and the scope maneuvered into the duodenum. A flexible snare was passed through the accessory channel of the scope and attached to a custom capsule deployment pod to permit delivery of capsule into the duodenal lumen along with 5–15 mL of water. After completion of the infusion, the scope and delivery devices were removed and all animals recovered well. Systemic blood was collected (~500 μ L) predosing, 2, 4, 24, 48, and 96 h, 1 and 2 weeks postprocedure.

Oral delivery of the enteric-coated capsules filled with either titanium oxide or mAb in the same monkeys ($n = 6$) while awake and restrained was facilitated by encouraging them to drink Tang. All monkeys were first dosed with titanium-filled capsules and X-rayed 4 h later to confirm that the intact capsule was not retained in the stomach and dissolution had occurred (no dense capsule could be visualized). For repeated dosing of mAb-filled capsules, systemic blood samples were collected predose, 24, 48 and 72 h later.

Detection of full-length mAb

Serum samples were analyzed for full-length mAb based on the MesoScale Discovery (MSD, Rockville, MD) electrochemiluminescent format as reported previously (Hornby et al. 2014). In brief, an anti-idiotypic antibody specific to anti-RSV was labeled with Sulfo-NHS-LC-Biotin and used as capture antibody on streptavidin-coated MSD plates. A pan anti-human IgG1/IgG2 antibody labeled with MSD Sulfo-TAG NHS Ester was used as the detection antibody. Relative luminescent units (RLU) were measured using an MSD plate reader (Sector Imager 6000) and Discovery Workbench software (MSD, Rockville, MD). For beagle and cynomolgus, the assay was assessed in serum collected from the same animals using spiked samples and standard curves to determine the LLOQ. Acceptance criteria were a minimum of twofold over background signal: noise ratio for samples, and 70–130% recovery on spiked QC duplicates. Sample concen-

trations were back-calculated by extrapolation from the standard curve (0.05–500 ng/mL) based nonlinear regression analysis of standard curves (GraphPad Prism (La Jolla, CA) version 5).

Monoclonal antibody proteolysis

Stability of mAb was determined *in vivo* after direct intestinal administration of mAbs in isoflurane-anesthetized c57b/6 mice, as described previously (Kliwinski *et al.* 2013). After 90 min, animals were killed and 5 cm of distal small intestine rapidly removed. The contents were diluted 1:1 in monkey serum containing protease inhibitor and centrifuged (1500 g for 10 min). Supernatants were stored frozen (−90°C) until analysis for full-length mAb.

Cynomolgus intestinal contents (1 donor, Bioreclamation/IVT, NY) were centrifuged (15 or 50 mL conical tubes 480 g 5") and supernatants obtained from ileum specimens. There was insufficient fluid from duodenum and jejunum samples. The ileum supernatant (centrifuged 20 000 g 5" 2X) was aliquoted and stored (−80°C). For cynomolgus ileum fluid digest, IgG2 and IgG1 mAb (~200 µg) were digested separately in 20 µL supernatant at 37°C. For each antibody, sample timed digestions (0–60 min) were stopped with an equal volume ice cold DPBS pH 7.2 (Dulbecco's Phosphate Buffered Saline, Gibco) containing protease inhibitors (Roche).

IgG1 and IgG2 fragments were purified with protein A/L resins mix. Protein L and protein A capture was based on 10 µg IgG to 1 µL resin, and 30 µg IgG to 1 µL resin, respectively. Digest material (50 µL) were incubated with resins (2 h at RT) and mixed with gentle rotation. Resins are washed 5× W/cold binding buffer ~400 µL each by centrifugation as above. To each resin, 40 µL of elution buffer (0.1 mol/L glycine-HCl, pH 2.8) was added for 10 min with intermittent mixing while kept on ice. Supernatants were collected from resin after wash, centrifuge, and elution (0.1 mol/L glycine-HCl, pH 2.8), and centrifuged again then stored at −80°C. In addition, after digestions, an antiidiotype antibody was used to capture mAb followed by either assay ruthenylated R10Z8E9 for anti-hFc detection or ruthenylated mouse anti-hKappa at 500 ng/mL for anti-kappa detection to differentiate full-length mAb and Fab remaining quantified by MSD RLU back-calculated to concentrations, as above.

Gel electrophoresis/Coomassie stain used 30 µL samples with 1.5 µL of running buffer (NuPage Tris Acetate SDS 20× Running Buffer) and 10 µL LDS sample buffer (NuPage LDS Sample Buffer 4X). Control IgG fragments (5 µL) of IgG1, Fc without core hinge, Fab papain, Fc papain, IgG fragments were prepared in-house. All sam-

ples and controls, but not molecular weight markers (Novex Sharp Prestained protein standards), were heated at 100°C for 5 min in sand block. A gel apparatus (Invitrogen (Carlsbad, CA) XCell4 Surelock Midi-cell) was prepared, loaded (20 µL samples; 10 µL molecular weight markers and controls), and run at 150 V (constant) for 60 min. After rinsing, InstantBlue (Expedeon San Diego, CA) was added for 15–20 min, further rinsed, and scanned (Hp Scanjet 7400c).

IgG1 and IgG2 protease digestion was also performed in human simulated intestinal fluid, and after IgG SDS gel electrophoresis was quantified by Odyssey Infrared Imager (Li-Cor Biosciences, Lincoln, Nebraska). Fasting Simulated Small Intestinal Fluid (FaSSIF) was made to mimic duodenal conditions of pH of 6.5 with an osmolality of approximately 270 mOsmol/kg, and included: NaH₂PO₄ (3.9 g), NaOH (to pH 6.5), sodium taurocholate (3 mmol/L), lecithin (0.75 mmol/L), and NaCl (3.093 g) in dH₂O (1 L). To this was added 100 µg/mL trypsin, 100 µg/mL chymotrypsin, and 300 µg/mL elastase in a total volume of 50 µL. Western blot was performed on samples, digested over 3 h and containing 1 mg/mL of each antibody and 200 ng of protein and detection was performed using anti-IgG(H + L). Purified fragments of IgG Fc with hinge region, Fab, and Fc without hinge aided in the identification of digestion products.

In addition to wild-type (WT) IgG1 and IgG2, chimeric antibodies were engineered. The sequence in IgG1WT upper hinge was engineered at EU# 233–235 ELL → PVA, which was expected to be a proteolytically resistant portion of the IgG2WT hinge region. An additional mutation was included at 239 (S→D) to reduce ides cleavage, which was less important for this study. The core hinge sequence of IgG1 and IgG2 are conserved (EU# 226–229 = CPPC) but the sequences are different in the upper and lower hinge, therefore, in a second chimeric IgG1, the complete hinge of IgG2 heavy chain was engineered into IgG1 (EU# 217–235 = TVERKCCVECPAPPVA).

Chemical physical mAb characteristics, formulation lyophilization, and milling

mAb FcRn Affinity

A variant (termed IgG2 M428L) was generated by mutating a methionine at position 428 to leucine IgG2 M428L (Shields *et al.* 2001). FcRn binding affinity was determined by surface plasmon resonance at pH 6.0 for IgG2 M428L that was taken from the original batch in PBS (release), lyophilized, milled after encapsulation. A ProteOn XPR36 GLC biosensor chip (Bio-Rad, Hercules, CA) was preconditioned with 0.5% sodium dodecyl sulfate (SDS),

50 mmol/L NaOH, and 100 mmol/L HCl in both the vertical (ligand) and horizontal (analyte) channels. Following equilibration with PBS-TE running buffer (20 mmol/L Na-phosphate, 150 mmol/L NaCl, 0.005% Tween-20, 3 mmol/L EDTA, pH 6.0), FcRn was immobilized using an amine coupling kit at a temperature of 25°C and a flow rate of 30 μ L/min. All channels were activated with a mixture of EDC (0.2 mol/L) and sulfo-NHS (0.05 mol/L) at 30 μ L/min for 4 min, followed immediately by immobilization of rat FcRn (3 μ g/mL in 10 mmol/L sodium acetate pH 4.5) over channels 1 and 2 at 30 μ L/min for 5 min. The reference channel was treated identically without injection of FcRn. All channels were then blocked for 5 min with an injection of 1 mol/L ethanamine-HCl (pH 8.5). This method resulted in cynomolgus FcRn coupled at response levels of 193 and 161 RU (1 RU = 1 pg protein/mm²) in channels 1 and 2, respectively. Following immobilization, IgG2 M428L samples were diluted with running buffer formulated at pH 6.0. Each mAb was tested at five concentrations in duplicate using a fivefold dilution series. The five concentrations of each analyte were injected simultaneously at a flow rate of 60 μ L/min for a 1 min association phase which was followed by a 3 min dissociation phase. The surface was regenerated prior to each subsequent mAb and tested with two injections of sodium phosphate (pH 8.0) followed by one injection of running buffer (pH 6.0). Affinity analysis and kinetic constants were calculated from the sensorgrams using the bivalent analyte model of the Proton XPR36 software.

Preformulation

About 10 g of IgG2 M428L was manufactured (Sino Biologicals Inc., Beijing, China). The mAb purity (>95% monomeric) was analyzed and confirmed by size exclusion chromatography and gel electrophoresis. Protein concentration was determined by ultraviolet (UV) absorption spectrophotometer at 280 nm using an extinction coefficient of 1.44L g/cm. The mAb used in this study is a human immunoglobulin G (IgG), isotype 2.

For preformulation studies, IGG2 M428L was extensively dialyzed into respective buffers (Step 1; Fig. 3): 20 mmol/L potassium phosphate, pH 7.5; 20 mmol/L potassium phosphate, pH 7.0; 20 mmol/L histidine, pH 6.5; 20 mmol/L histidine, pH 6.0; 20 mmol/L histidine, pH 5.6; 20 mmol/L sodium acetate, pH 5.3; and 20 mol/L sodium acetate, pH 5.0.

Differential scanning calorimetry

Differential scanning calorimetry experiments were performed on a MicroCal's Auto VP-capillary DSC system in

which temperature differences between the reference cell (containing respective buffer blank) and sample cell (containing protein in respective buffer) was continuously measured and calibrated to power units. Samples were heated from 20°C to 95°C at a heating rate of 60°C/h and heat capacity change was measured. Prescan time of 15 min and a filtering period of 10 sec were used for each scan. DSC measurements were made at about 0.5 mg/mL. Analysis of the resulting thermograms was performed by using MicroCal Origin 7 software (Northampton, MA).

Dynamic light scattering

Particle sizes and distributions of samples were determined on a DynaPro Plate Reader Dynamic light scattering (DLS) instrument (Wyatt Technologies Corporation, Santa Barbara, CA). Measurements were made using a Corning[®] 384-well black plate with clear flat bottom polystyrene (CLS3540) with 40 μ L sample in each well at 1 mg/mL IGG2 M428L concentration in respective buffer. For each candidate, duplicate measurement is made, and for every measurement 20 runs are performed. DLS thermal ramp experiment was performed at 25°C and the instrument was programmed to ramp to 71°C. DLS measurements were made between 25°C and 71°C.

PEG -induced protein precipitation method

This was used to determine the relative solubility of protein in different buffer and pH conditions. Polyethylene glycol (PEG) precipitation experiments were performed in a 96-well plate format in which B21M huIgG2 mAb samples were mixed with PEG 6000 stock solutions in respective buffer to achieve final protein concentration of 1 mg/mL and PEG concentration ranging from 0% to 36% (w/v). The mixing was performed on a 96-well filter plate with 0.2 μ mol/L size pores (Pall Part # 5029). After mixing, the 96-well plates with protein and PEG 6000 at varying concentration was incubated for 2 h on a shaker at room temperature. After incubation time, these plates were placed on corresponding 96-well UV-VIS receiving plates (Corning Part # 3639) followed by centrifugation at 480 g for about 20 min to collect soluble protein in the receiver plate. These receiving plates were directly placed in a plate reader (Molecular Devices M5 spectra Max plate reader) for absorbance measurements to determine protein loss due to precipitation during the overnight incubation.

The 40% PEG 6000 stock solutions in different buffers were prepared by adding 5 mL of 200 mmol/L buffer to 40 mL of 50% PEG 6000 solution followed by adjusting pH by adding 1 mol/L HCl or NaOH to get desirable pH. After pH adjustment samples were made to 50 mL volume by adding deionized water.

Accelerated stability studies

IgG2 M428L was extensively dialyzed into 20 mmol/L histidine, pH 6.5 with 8.5% sucrose; 20 mmol/L histidine, pH 6.0 with 8.5% sucrose; 20 mmol/L histidine, pH 5.5 with 8.5% sucrose; and 20 mmol/L acetate, pH 5.3 with 8.5% sucrose. After dialyses, samples were concentrated to about 55 mg/mL using Amicon® (Sigma Aldrich, St. Louis, MO) Ultra 15 mL Centrifugal Filters. Following concentration, the concentration of the samples was adjusted to about 50 mg/mL by addition of respective buffer. A 4% (w/v) PS80 stock solution in water was used to make the final PS concentration of 0.04% in each sample. Samples were sterile filtered using 0.22 µmol/L filter. The filtered protein in respective buffers were filled into prewashed and sterilized 2R size vials (SCHOTT; Item # 54520) and closed with sterilized Daikyo stopper (SERUM S10-F451 RSV). The filled vials were crimped with aluminum caps and stored in respective incubators for up to 4 weeks. Samples were analyzed at time, T = 0 week, at T = 1 week incubated at 4°C and 40°C and T = 4 weeks incubated at 4°C and 40°C. At each time points samples were removed from the incubator and analyzed for visible particles by visual inspection against black and white background, turbidity by absorbance at 350 nm, concentration by absorbance at 280 nm; SDS-PAGE (reduced and nonreduced), SEC and DLS for soluble aggregates, and MSD for bioassay.

Lyophilization

IgG2 M429L mAb was dialyzed and concentrated to approximately 50 mg/mL in 10 mmol/L histidine pH 5.7 with 8.5% (w/v) sucrose by an ultrafiltration (UF)/diafiltration (DF) process using a Millipore LabScale TFF system with Millipore 30 kDa Biomax UF/DF membranes. A 4% (w/v) PS80 stock solution in water was used to make the B21M huIgG2 mAb formulated bulk (FB) with 0.04% (w/v) PS80. The FB was sterile filtered using a PVDF filter unit (0.2 µmol/L pore size). Buffer blank (without mAb), 10 mmol/L histidine, pH 5.7 with 8.5% sucrose and 0.04% PS80 was also prepared and sterile filtered using a PVDF filter unit (0.2 µmol/L pore size).

Approximately 2.2 mL of filtered IgG2 M428L FB was filled in 8R BB Type 1 prewashed and sterile glass vials (Fiolax clear, SCHOTT forma Vitrum). Similarly, 2.2 mL of buffer blank was added to the 8R vials. The vials were capped with Daikyo Seiko caps (Formular: D777-1; Coating RB2-TR) with partial opening.

Freeze drying was conducted using a Virtis Genesis Lyophilizer (SP Scientific, Stone Bridge, NY) (S/N: 216734). Filled vials were placed into bottomless stainless steel lyophilization trays and transported to the lyophili-

zer after the completion of the filling operation. The tray was placed on precooled shelf at 5°C. After a hold time of 30 min at 5°C, shelf temperature was changed to -50°C by ramping the temperature down at 0.4°C per min. The shelves were maintained at this temperature for about 3 h to allow sufficient time for all samples to freeze completely. After freezing, the temperature was ramped up to -15°C (at 0.4°C per min) and primary drying was conducted for about 48 h at a chamber pressure of 100 mTorr (0.133 mbar). After completion of primary drying, the shelves temperature was ramped to +35°C (at 0.4°C per min) and secondary drying was performed for 10 h. After secondary drying was complete, the shelf temperature was ramped to 25°C (at 0.8°C per min), followed by lowering of the chamber pressure to 525 Torr. The vials caps were completely closed under vacuum. The chamber pressure was then completely released and the sample tray was removed from the lyophilizer. The lyophilized vials were stored at 4°C.

Milling

Lyophilized cake in 8R vials were gently broken into smaller pieces with a sterile spatula and transferred to a 50 mL precleaner and sterilized porcelain mortar (70 mm × 47 mm; VWR Catalog # 89038-144). Small pieces of lyophilized cake were gently crushed with a corresponding pestle (VWR catalog # 89038-160) into fine powder and extensively mixed. Milled material was transferred into a 30R vials (previously washed and sterilized) and the vials were crimped and stored in plastic bags at 4°C before filling in capsules.

Residual moisture measurement

The residual moisture content of the freeze dried and milled product was measured by the Karl Fisher titration method using a Brinkmann™/Metrohm™ Models 756 Coulometric Karl Fischer Titrators. Conditioned hydranal (Hydranal Coulomat AG; Fluka Catalog # 34836) was added to the freeze-dried product or milled product and mixed by vortexing for 30 sec. The mixture was allowed to sit for 2 h, after which sample moisture was determined by adding 8 mL of the hydranal from the sample vial into the test vessel.

Filling of the capsules

Hard gelatin capsules sizes 3 were filled with 54 mg of milled IgG2 M428L and closed. The closed capsules were coated with an intermediate layer of hydroxyl propyl cellulose (HPC) and an enteric top layer of hypoxypromethyl cellulose acetate succinate (HPMCAS)-HF

(13 mg/cm²). HPMCAS polymer was used as the enteric film coating because it is insoluble in acidic condition, but readily swells and dissolves in aqueous environment. Additionally, 20 titanium oxide filled capsules were prepared with HPMCAS coating (13 mg/cm²) and used to determine that passage of this size passes through the pylorus within 4 h by X-ray.

Enteric-coated dissolution studies

Dissolution studies of IgG2 M428L filled enteric-coated capsules were performed using a dissolution test system with apparatus 2 (paddle). Dissolution of 5 capsules each was tested in 500 mL of 50 mmol/L phosphate buffer at pH 7.5 and pH 6.5, respectively. Capsule sinkers were used to keep the capsule submerged in buffer.

Results

mAb proteolysis

The stability of IgG1 and IgG2 mAb isotypes in intestinal fluid from different sources was compared by a variety of methods and quantified where possible (Fig. 1). A representative western blot (Fig. 1A) illustrates rapid fragmentation of IgG1WT within 5 min after incubation in combined intestinal proteases (in FaSSIF with 100 µg/mL human pancreatic trypsin and chymotrypsin, and 300 µg/mL porcine pancreatic elastase). In contrast IgG2WT fragments <60 kDa were not resolved within the 3 h digestion period. This was also the case for IgG2WT during a chymotrypsin digestion (100 µg/mL chymotrypsin in FaSSIF), where the identity of the IgG1 WT fragments is indicated by their migration consistent with an Fc fragment containing the core hinge and two identical Fab fragments (Fig. 1B). This suggests that cleavage was in the upper hinge region (Medgyesi et al. 1973), at least initially. The dashed box in Figure 1A indicates fragments that were N-terminally sequenced, which identified cleavage between positions K222 and T223. Therefore, engineered IgG1 antibodies were created with residue changes at the enzyme's cleavage point an IgG1 using a proline substitution at K222 in an attempt to confer protease resistance. This strategy was not successful and engineered mAb was rapidly digested (data not shown), as was an IgG1 chimeric with IgG2 EU# 233–235 PVA substitution. However, an engineered IgG1 chimeric with complete IgG2 hinge region (positions 217–235) was resistant to cleavage after trypsin digestion compared to IgG1WT and more similar to IgG2WT over the 3 h time period (Fig. 1B far right).

Digestion of IgG1 and IgG2WT in intestinal fluid samples taken from cynomolgus ileum was performed to more closely mimic the *in vivo* studies and the protein

detected by Commassie blue stain. Although this method is less sensitive than western Blot (10–25 ng detection vs. 10–100 pg) it confirmed the above data by detecting the fragments that included Fc with core hinge (50 kDa) and fAb (45 kDa) within 30 min for IgG1, whereas IgG2 was mostly intact up to 60 (Fig. 1C). To attempt to quantify the effects of trypsin digestion of IgG1WT and IgG2WT, the intact antibody bands from western blots were quantified for each time point using an Odyssey Infrared Imager. Figure 1D confirms that no full-length IgG1WT antibody remains after the 5 min of digestion with trypsin, whereas ~50% of full-length IgG2 remains, declining to about 25% of the intact antibody at 3 h. Full-length IgG2 detection was compared to IgG1 in mice 90 min after *in vivo* intraileal administration under isoflourane anesthesia (Fig. 1E). This single time point was selected based on our previous sampling of intestinal fluid 90 min after intrainestinal IgG1 dosing in neonatal rat pups (Kliwinski et al. 2013) and cynomolgus monkey (Hornby et al. 2014). In the latter case, we noted that if mAb level in intestinal fluid was lower than 1000 ng/mL 90 min after direct intestinal infusion then negligible serum levels were detected in those monkeys. Ninety minutes after intrainestinal dosing, half the mice had IgG2 concentrations in ileum that were above 1000 ng/mL and were on average ~100-fold higher concentration compared to IgG1 (Fig. 1E). The illustrated scatter plot suggests that the IgG2 was still susceptible to proteases present in half the animals dosed into the intestine.

Digestion of IgG1 and IgG2 was also compared over time in intestinal fluid isolated from cynomolgus ileum and quantified by MSD where capture was by antiidiotype and detection at either the fAb (anti-kappa mAb) or full-length mAb (anti-Fc mAb). Detection by Fc region illustrated that 12% intact IgG 1 was present at 30 min declining to 3% at 60 min whereas a majority of IgG2 was still present as full-length mAb at 60 min (57.4%; Fig. 1F).

Based on the proteolytic stability of IgG2 involving the complete hinge region, a IgG2 mAb was selected for oral delivery. An IgG2 variant (termed M428L) was generated with an Fc mutation involving a methionine at position 428 to leucine (Zalevsky et al. 2010) for binding affinity to cynomolgus FcRn at pH 6.0. We previously reported an ~2-fold increase in affinity based on antigrowth factor IgG2 (Hornby et al. 2014). The antirespiratory syncytial virus (RSV) mAb was selected for generating the IgG2 FcRn high affinity variant to avoid potential binding of mAb to an endogenous cynomolgus ligand other than FcRn. The binding affinity of the recombinantly generated batch (in PBS) to cynomolgus FcRn at pH 6.0 was measured directly by surface plasmon resonance and $K_D = 191 \pm 5.66$ nmol/L (mean \pm SD; $n = 3$) obtained. A similar binding affinity was determined for the mAb

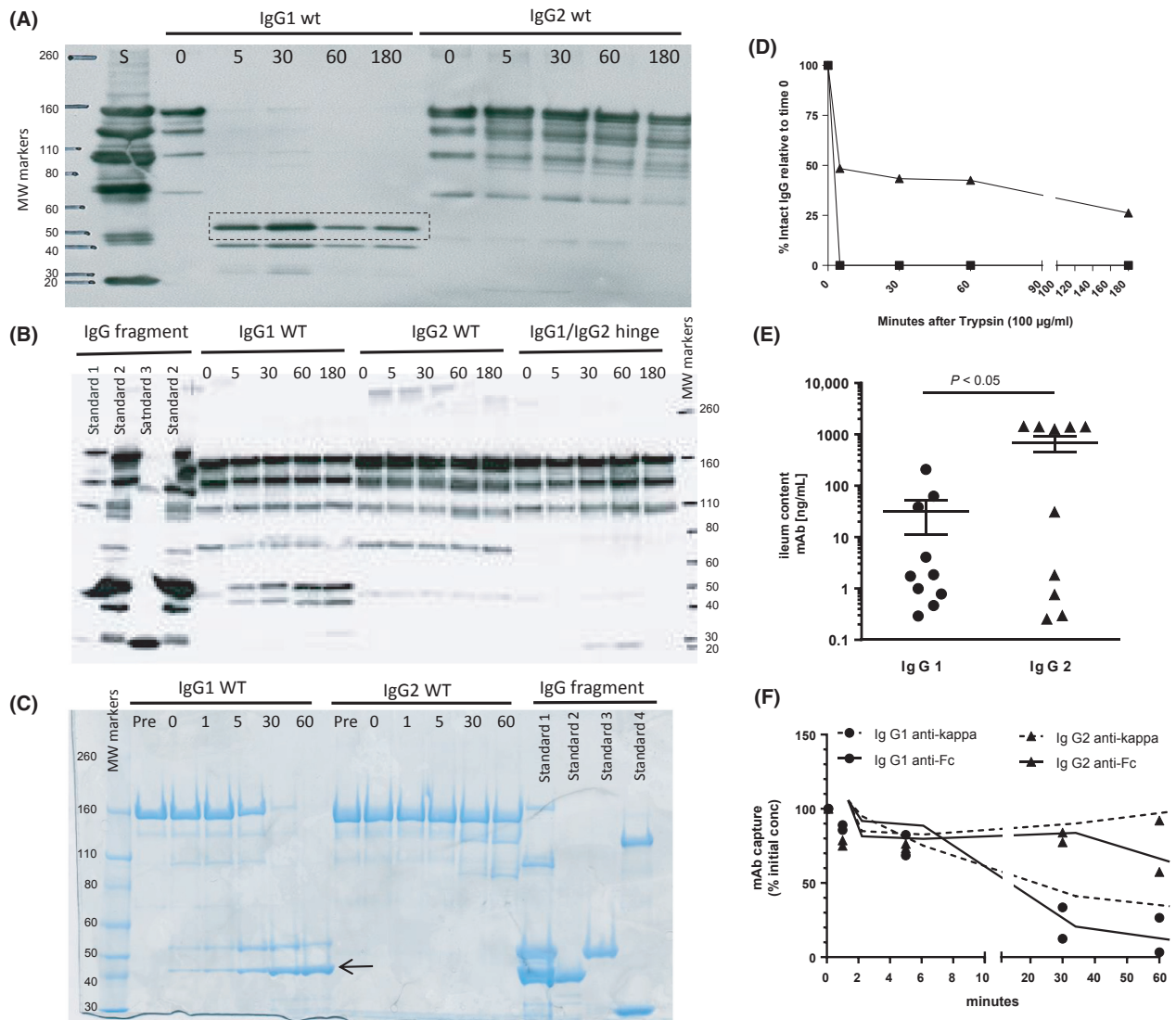


Figure 1. (A). Western blot of IgG1WT and IgG2WT samples during combined protease digestion up to 3 h (in FaSSiF pH 6.5 with 100 μ g/mL human pancreatic trypsin, 100 μ g/mL human pancreatic chymotrypsin, and 300 μ g/mL porcine pancreatic elastase for 3 h). The dashed indicates fragments that were N-terminally sequenced to indicate cleavage at K222. (B). Digest (100 μ g/mL human pancreatic chymotrypsin in FaSSiF) of IgG1WT, IgG2WT and an engineered IgG1 chimeric with complete IgG2 hinge region (positions 217–235) with standards: 1 = F(ab')₂, ScIgG, Fc without core hinge; 2 = IgG1 intact, IgG1 Fab, IgG1 Fc with core hinge; 3 = IgG1 Fc without core hinge. (C). Digestion of antibodies in cynomolgus intestinal fluid followed by Comassie blue stain illustrates where the majority of IgG1 is digested into fragments that included Fc with core hinge (50 kDa) and fAb (45 kDa), whereas IgG2 is mostly intact IgG (150 kDa) up to 60 min Standards: 1 = IgG1 F(ab')₂, Fab, Fc w/core; 2 = Fab papain CTE3; 3 = Fc papain CTE3; 4 = IgG1 Fc w/o core hinge. (D). Units of absorbance (Odyssey Infrared Imager) illustrated as % intact of IgG1 WT and IgG2 WT during trypsin digestion (100 μ g/mL in FaSSiF pH 6.5, 37°C) up to 3 h confirms complete loss of IgG1 within 5 min, whereas IgG2 is relatively stable. (E). Digestion in mouse intestine *in vivo* illustrates that levels of full-length IgG2 > IgG1 detected in ileum fluid sampled 90 min after ileum delivery of 1 mg/kg of either isotype in c57b/6 mice $P < 0.05$ by unpaired *t*-test. (F) IgG1 (filled circle) compared to IgG2 (filled triangle) quantification of presence full-length mAb was confirmed after digestion in samples of cynomolgus intestinal fluid by MSD/ELISA where an antiidiotype antibody was used to capture then detection were either by antibodies against the fAb κ chain (dashed line representing total with fAb – either fAb alone or up to full length) or terminal Fc region (solid line, representing full-length mAb only).

after lyophilization and milling $K_D = 167 \pm 6.00$ nmol/L (mean \pm SD; $n = 3$) and in mAb dissolution from enteric-coated capsules $K_D = 205 \pm 7.51$ (mean \pm SD; $n = 3$).

Cynomolgus intestinal pH profiling

Prior to formulation, lyophilization and encapsulation of IgG2 M428L, we profiled the cynomolgus intestine for the

pH appropriate for enteric-coating for intestinal site-specific release and avoidance of gastric exposure. Based on our previous work in cynomolgus, release of capsule content in the distal small intestine was preferable (Hornby et al. 2014). Human studies indicate that, after exiting the stomach at ~pH 2, small intestinal pH increases from ~6 at the duodenum to ~7.5 in distal small intestine (Evans et al. 1988). There were no literature reports of the pH of the cynomolgus intestine; therefore operator-assisted monitoring of IntelliCap System[®] capsules (size 000) was used to profile the intestinal pH for site-specific release of enteric-coated capsules. Table 1 illustrates the GI transit information in 3/6 fasted monkeys where the capsule passed the pyloric sphincter but with prolonged gastric residence times from 14 to 250 h, whereas normal gastric emptying in primate is within 4 h. Once in the small intestine, transit time was within the expected range for 2–3 h. In the other three monkeys gastric retention times ranged from 284 to 321 h before recording was no longer possible. In one monkey, the capsule was regurgitated, noted as a rapid increase in pH and immediately recovered by a handler from the cheek pouch of the animal at the time indicated. Examples of gastric emptying time, intestinal pH, and temperature are illustrated for a period of time for subjects #3 (Fig. 2A) and #4 (Fig. 2B). The capsule transits the pylorus 251 and 19 h after dosing, as shown by the rapid rate of rise of pH. In both individuals, there is a sustained pH at above pH 7 which continues to rise during small bowel transit to pH 8.5 over the course of the next 2 h, and then drops to pH 6.5 as the capsule enters the cecum/large intestine. Temperature fluctuations during gastric retention (Fig. 2A) represent eating/drinking periods and terminal drop in temperature

Table 1. Transit time (hours.min) based on IntelliCap System[®] monitoring in fasted monkey and dog

	Gastric residence	Small bowel transit	Total transit time
Subject (monkey) #			
1	—	—	121.23 ¹
2	—	—	>290
3	251.24	2.40	>284
4	19.03	3.16	32.36
5	14.19	2.23	141.47
6	—	—	>321
Subject (dog) #			
1	0.13	1.11	20.42
2	1.45	1.14	23.05
3	0.58	1.45	21.26
4	0.24	2.15	21.04
5	19.12	2.48	42.36
6	2.18	1.16	12.27

¹voided by mouth.

represents excretion (not shown). To attempt to improve gastric emptying of the capsules, three additional monkeys were fed immediately prior to dosing with IntelliCap System[®] capsules (size 000) orally; however, capsules were retained in the stomach in all three individuals.

Based on the variable gastric retention of these capsules in cynomolgus, we did not pursue dosing mAb using IntelliCap System[®] capsules. Instead, male beagles were dosed using IntelliCap System[®] ($N = 6$, ~3 mg/kg mAb in 170 μ L PBS) after overnight fasting, with food resumed 4 h after dosing. Burst release (12 min) was accomplished upon operator command by monitoring pH profile such that release of mAb was triggered 1 h after passage through the pylorus. As shown in Table 1 gastric emptying of the capsule occurred within the 4-hour fasting period in 5/6 subjects and capsules were successfully triggered to deliver in the mid to distal small bowel. In these dogs, serum was collected up to 96 h after dosing.

The MSD assay conditions were successfully optimized in beagle dog serum, but in this case the lower level of quantification was 1.0 ng/mL although the mAb was detected above background to 0.01 ng/mL. Based on this 4 of 6 dogs had no detectable serum levels up to 96 h after delivery. In the other two cases, their serum had background interference that gave false detection of mAb at $t = 0$ and were uninterpretable. We did not clone and expressed dog FcRn in order to determine an affinity of human IgG2 M428L variant, and abandoned the idea of testing oral administration of lyophilized mAb in enteric-coated capsules in this species.

mAb formulation, lyophilization, and capsule enteric coating

Figure 3 outlines the formulation development plan, a four-step strategy, for the selection of stable formulation conditions in which IgG2 M428L can be lyophilized, milled into small particles, and filled into gelatin capsules which can then be enterically coated and stored at 4°C until dosed. In steps 1 and 2, preformulation studies were performed to screen the physical–chemical properties of IgG2 M428L from a wide range of buffers and pH conditions to select a stable formulation buffer for lyophilization, milling, and oral delivery. In step 3 and 4, a lead formulation was selected, and lyophilization and milling was performed followed by analytical testing of reconstituted IgG2 M428L for aggregation and molecular integrity.

In the first step IgG2 M428L was screened in 7 buffers: 20 mmol/L potassium phosphate, pH 7.5; 20 mmol/L potassium phosphate, pH 7.0; 20 mmol/L histidine, pH 6.5; 20 mmol/L histidine, pH 6.0; 20 mmol/L histidine,

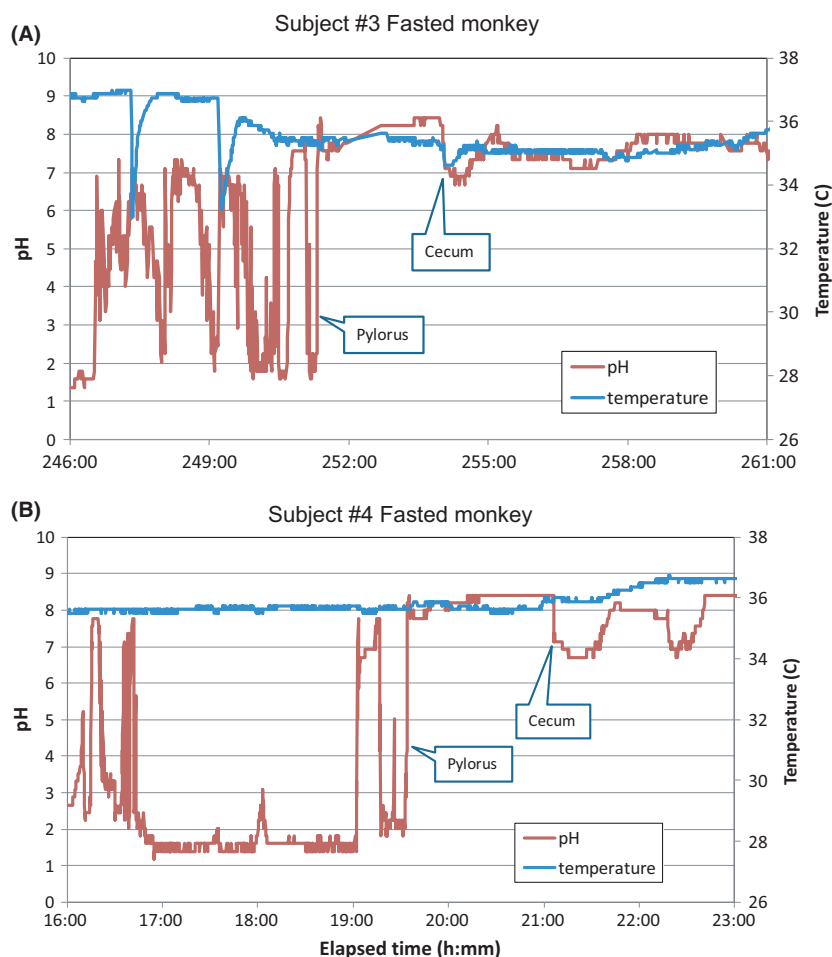


Figure 2. Ileal pH for site-specific release of enteric-coated capsules was determined in monkeys orally dosed with empty IntelliCap™ capsules (size 000) and illustrated for subjects 3(A) and 4(B). A rapid rate of rise of pH above 7 at the pyloric sphincter is sustained ~2 h indicating small intestinal transit time in both monkeys who had very different gastric retention times. Peak small intestinal pH at the ileum was pH >7.5 before decreasing to <pH6.5 in cecum and large intestine.

pH 5.5; 20 mmol/L sodium acetate, pH 5.5; and 20 mmol/L sodium acetate, pH 5.5.

Thermal stability of IgG2 M428L in all 7 buffers was determined by DSC. DSC is a thermodynamic method that measures the heat capacity changes of proteins as a function of temperature and provides information about conformational stability and structural integrity of proteins. The midpoint of thermal transition, T_M , was determined from the thermal denaturation profiles of IgG2 M428L in each buffer (Data not shown). The DSC scans of IgG2 M428L from 20°C to 95°C in different buffers did not show significant difference in the T_M value suggesting little or no conformation changes occurs when the protein is the pH range from 7.5 to 5.0.

Particle sizes and distributions of IgG2 M428L samples in respective buffers were determined by DLS at 25°C and after temperature ramp to 71°C. No change in

hydrodynamic radii (R) and % mass was detected at both temperatures 25°C and 71°C in all 7 buffers (data not shown).

Polyethylene glycol (PEG)-induced protein precipitation method was used to determine the relative solubility of protein in different buffer and pH conditions. PEG is a water soluble synthetic polymer. When proteins are added to the PEG solution they are excluded from the regions of the solvent occupied by PEG and are concentrated until the solubility is exceeded and precipitation occurs (Atha and Ingham, 1981). PEG-induced protein precipitation method showed IgG2 M428L has relatively higher apparent solubility in the pH range 5.0–5.5 and relatively lower solubility at higher pH. Based on these results, 4 buffers were selected in the pH range 6.5–5.3 for in vivo stability of IgG2 M428L at 50 mg/mL (step 2 in Fig. 3). In the second step, solution stability of IgG2 M428L mAb

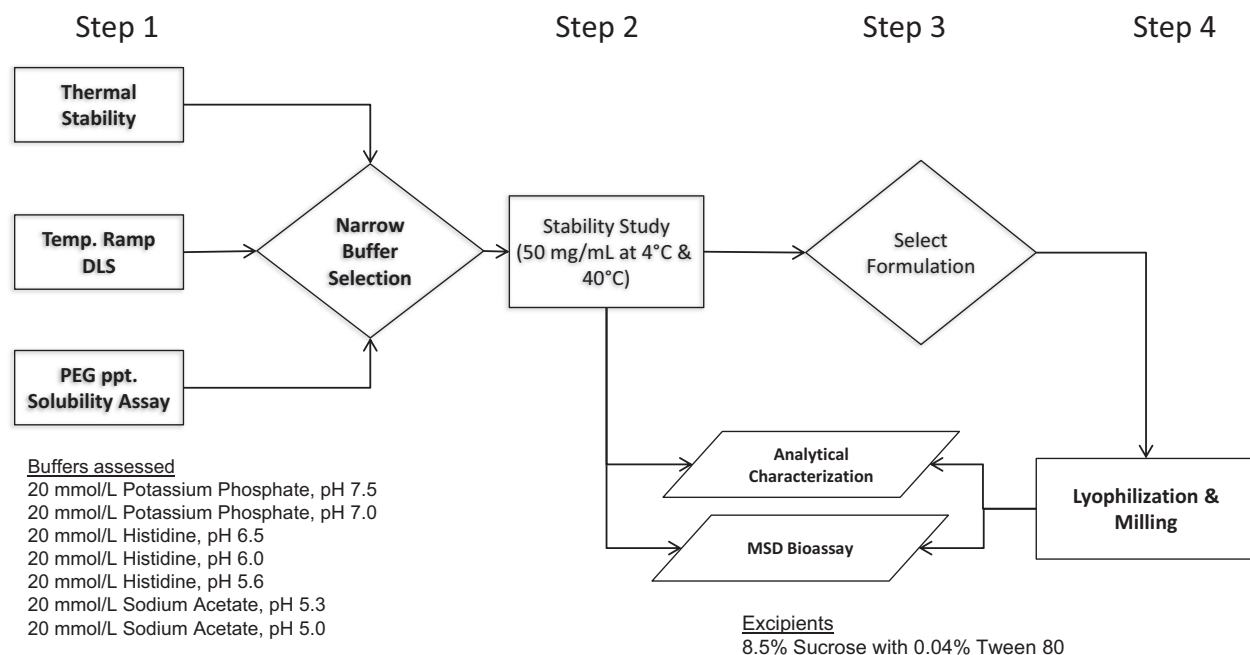


Figure 3. Steps involved in preformulation buffer selection, formulation and characterization of IgG2 M428L physical-chemical properties. Preformulation (Step 1) explored a wide range of pH & buffer conditions with a narrow range of pH buffers selected for stability (Step 2). In step 3 and 4, a lead formulation was selected and lyophilization and milling was performed followed by analytical testing of reconstituted mAb for aggregation and molecular integrity

at 50 mg/mL was tested by incubating mAb in accelerated stress condition at 40°C and refrigerated condition at 4°C for up to 4 weeks in buffers in the pH range 6.5–5.3 and at each time point analyzed by visual inspection, turbidity, concentration by absorbance at 280 nm, SDS-PAGE, SEC, and DLS (data not shown).

IgG2 M428L at 50 mg/mL was determined to be stable at 40°C in all four buffers for at least 4 weeks by analytical methods. No particles were observed by visual inspection, no change in concentration as determined by absorbance at 280 nm and no significant aggregation as determined by SDS-PAGE, SEC-HPLC and DLS. Based on these results, 10 mmol/L histidine pH 5.7 with 8.5% (w/v) sucrose and 0.04% (w/v) PS80 was selected as the final buffer for lyophilization as it was in the midrange in which the solution stability was tested (pH 6.5 to pH 5.3). Finally, the formulated IgG2 M428L at 50 mg/mL was lyophilized in 10 mmol/L histidine pH 5.7 with 8.5% (w/v) sucrose and 0.04% (w/v) PS80. The lyophilized cake appearance was white solid with no sign of melt back. The lyophilized cake in 8R vials were broken into small pieces transferred to presterilized porcelain mortar and milled with a corresponding pestle. Lyophilized and milled IgG2 M428L mAb was reconstituted and tested for any process-related detrimental changes by analytical methods for molecular integrity and bioactivity.

No significant change in aggregation state (Fig 4A–C) was observed by turbidity measurement by absorbance at 350 nm/280 nm and 405/280 nm, SEC and DLS; nor loss of integrity of the full-length mAb by MSD assay (Fig. 4D) was noted for the lyophilized and milled batch, compared to the release mAb in PBS and unlyophilized formulated mAb in solution.

Enteric-coated capsule dosing

Since size 000 capsules based on IntelliCap System (R) dosing resulted in prolonged gastric retention in cynomolgus, a smaller size of capsule had to be chosen for oral dosing. A lyophilized control mAb was used to assess the amounts that could be loaded into different hard capsule sizes (Table 2). On this basis, size 3 was selected as the maximal size of hard gelatin capsule likely to pass through the pylorus, while allowing for a fixed dose (23.2 mg–3 mg/kg in a 6 kg monkey) similar to our previous study (Hornby et al. 2014) Initial lyophilization of a control mAb into cakes resulted in 35% recovery of lyophilized material in capsules. Therefore, hard gelatin capsules were loaded in a glove box with 54 ± 2 mg lyophilized material, of which 18 mg was IgG2 M428L. An additional 20 capsules were loaded with titanium oxide which allowed confirmation by X-

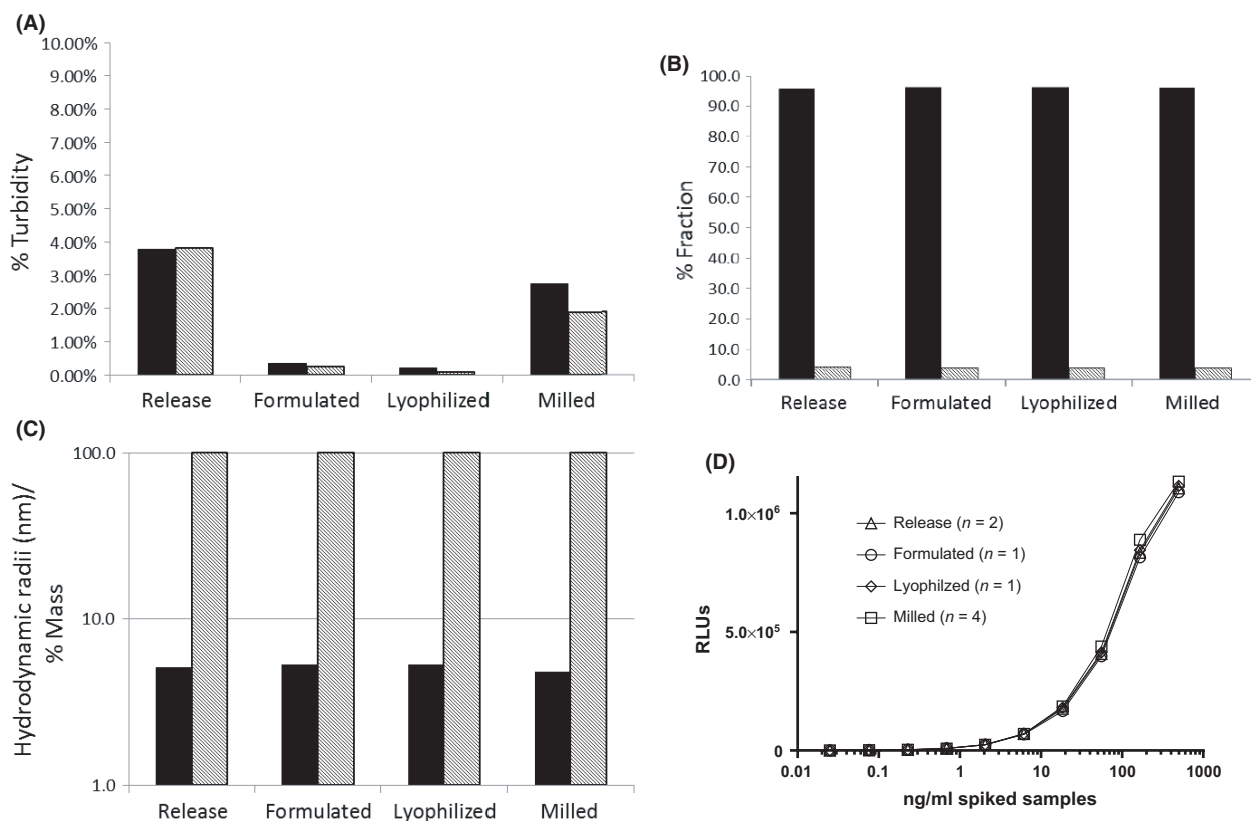


Figure 4. IgG2 M428L formulated and lyophilized in 10 mM histidine, pH 5.7, 8.5% sucrose, and 0.04% Tween 80 then hand-milled showed no significant change in aggregation state by (A). turbidity (B). SEC-UV and (C). DLS nor loss of molecular integrity by (D). Relative Luminescent Units (RLU) detecting no differences in full-length mAb by MSD (antiidotype capture and Fc detection in duplicate wells) using a range of concentrations of spiked mAb release batch in PBS ('release' is mean ± SEM of repeated experiments) compared to formulated (single experiment), lyophilized (single experiment), and milled (mean ± SEM four independent replicates) IgG2 M428L.

Table 2. Capsule size and volume of lyophilized mAb (active ingredient only)

Capsule size	Volume (mL)	mAb (mg)	Dosing/Capsule (6 kg monkey)
Control mAb Size 0	0.68	47.0	~7 mg/kg
Control mAb Size 1	0.50	37.9	~6 mg/kg
Control mAb Size 2	0.37	27.9	~4 mg/kg
Control mAb Size 3	0.30	23.2	~3 mg/kg
Test IgG2 Size 3	0.30	19.3	~3 mg/kg

ray taken 4 h after dosing to confirm passage through the pylorus and selection of monkeys to be dosed.

Dissolution was tested by measuring absorbance at 280 nm with a UV-VIS fiber optic probe submerged in the buffer. The IgG2 M428L filled enteric-coated capsules started breaking in ~ 75 min and 20 min, in pH 7.5 and pH 6.5 buffers, respectively. This is consistent with earlier observed dissolution time with coloring agent filled capsules. It took about 1 h to completely dissolve IgG2 M428L milled powder in pH 7.5 buffer with 98.2% recov-

ery and ~3 h to completely dissolve IgG2 M428L milled powder in pH 6.5 buffer with 95.7% recovery.

Eudragit® (Evonik industries, Essen Germany) coating was selected for enteric-specific release. To determine optimal enteric-coating thickness, placebo filled capsules were coated with either 4 or 13 mg/cm² HPMC-AS and dissolution times determined in different pH conditions (Table 3). While both coating thicknesses showed very slow dissolution at acidic pH that would be experienced in the stomach, the 4 mg/cm² dissolution was rapid (5 min) at pH 6.5 and the cynomolgus GI profile indicated that occasional pH 6 may be experienced in the stomach. In contrast, 13 mg/cm² HPMC-AS coating dissolution was over one hour at pH 6.5 and occurred within 20 min of exposure to pH 7.5, therefore this coating was selected to be consistent with small intestinal release. At the target pH the coating took 2–3 min to breakdown and gelatin dissolves in ~5 min which is similar to IntelliCap® System burst release of approximately 11 min. A total of 192 enteric-coated capsules were generated.

Table 3. Dissolution time of placebo release of HPMC-AS coating at different pH conditions

HPMC-AS coating (mg/cm ²)	Size 3 Hard gelatin capsule							
	pH 2.0		pH 4.5		pH 6.5		pH 7.5	
	(0.01N HCl)		(KH ₂ PO ₄)		(KH ₂ PO ₄)		(KH ₂ PO ₄)	
	caps1	caps2	caps1	caps2	caps1	caps2	caps1	caps2
4	100 min	>18 h	>10 h	>18 h	5 min	5 min	5 min	5 min
13	>18 h	>18 h	>18 h	>18 h	75 min	75 min	20 min	20 min

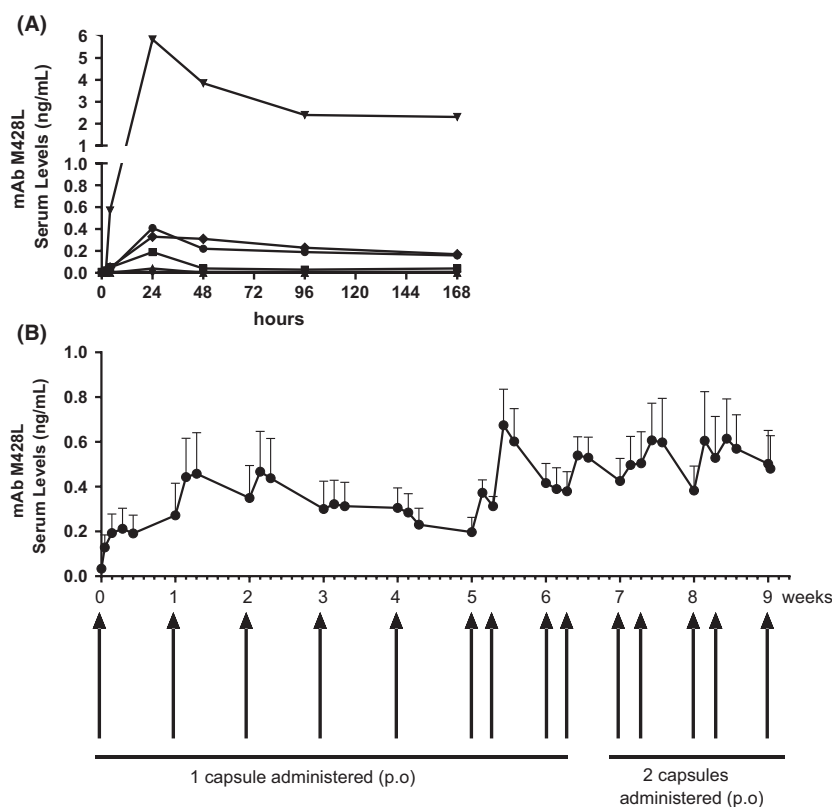


Figure 5. (A). Delivery of enteric-coated capsules containing 18 mg of IgG to the small intestine was ensured by endoscopic dosing with the capsule attached to a snare. Individual monkey mAb serum levels of mAb are low with peak levels at 24 h. (B). Serum levels following repeat oral IgG enteric-coated capsule dosing orally administered to o/n fasted conscious cynomolgus monkeys ($n = 6$). From weeks 1–5, one capsule was administered a week; on weeks 6 and 7, two capsules were administered a week 48 h apart; and during weeks 8, 9, and 10 two capsules were given simultaneously twice a week.

Initially, delivery of capsules was made directly into the small intestine by endoscopic dosing with the capsule attached to a specially engineered snare. Individual monkey serum levels of mAb (Fig. 5A) followed a similar time course of uptake to that of previous unformulated endoscopic delivery (Hornby et al. 2014), with peak levels at 24 h. However, serum levels for all but one monkey were <1 ng/mL. For reference, based on the weight (3.05–3.80 kg) of these female monkeys and their estimated blood volume (Ageyama et al. 2001) a 1% fractional

uptake of the 23.2 mg mAb orally delivered would be 954 ng/mL. Thus, the <1 ng/mL values are 1000-fold lower than a minimally acceptable 1% oral bioavailability after a single dose. Data from one monkey with higher levels should be viewed with caution since she bit the capsule during dosing and may have inhaled the lyophilized mAb. After exclusion of this monkey, mAb serum levels at 24 h were 0.20 ± 0.18 ng/mL (mean \pm SEM, $n = 5$).

To confirm gastric emptying of the size 3 capsule, and its dissolution in vivo, each of these monkeys was then

dosed orally with an identical titanium-filled enteric-coated capsule and X-rayed 4 h later. In each case the capsule which had apparently dissolved, with no evidence of gastric retention (data not shown). The same monkeys were then dosed with one mAb-filled capsule per week based on expected 14 day circulating half-life of a 0.05 mg/kg IV of an anti-growth factor mAb (Hornby *et al.* 2014). Serum mAb levels were tracked for 5 weeks, to determine if accumulation occurred and confirm whether the expected PK profile was consistent with the dosing schedule (Fig. 5B). Serum levels doubled to ~0.4 ng/mL in the second week of dosing, but this increase was not sustained in subsequent weeks. Further increasing the dose to one capsule biweekly, or two capsules biweekly, did not increase serum levels to levels above 1 ng/mL.

Discussion

These results, obtained by both endoscopic intestinal dosing and oral delivery of enteric-coated capsules containing lyophilized mAb, question the validity and feasibility of targeting FcRn expressed by enterocytes in adult primates to orally deliver and achieve intact mAb therapeutic circulating levels. The discussion will focus on the possible reasons for these results, in light of the efforts to select the antibody for FcRn binding affinity and protease resistance, and experiments to control for potentially confounding factors. These include confirmation of mAb biophysical properties and molecular integrity after processing, capsule size for passage through the pylorus in cynomolgus, and dissolution at the appropriate region of the small intestine.

In our previous acute dosing study, variable amounts of full-length IgG1 mAb (over several log units for $\mu\text{g}/\text{mL}$) had been obtained after 90 min in small intestinal fluid in cynomolgus *in vivo* (Hornby *et al.* 2014). In this study, an IgG2 isotype was selected that resisted intestinal enzyme proteolysis for longer than IgG1, which was the isotype used for direct intestinal infusion of mAb (Hornby *et al.* 2014). The protease resistance of IgG2 was confirmed *ex vivo* in fasted monkey intestinal fluid and *in vitro* in human FaSSIF containing digestive enzymes. These two methods mimicked the conditions in fasted human volunteer small intestinal fluid (de la Cruz Perez Moreno *et al.* 2006). The initial cleavage site was identified as K222 by N-terminal sequencing of the products of IgG1 digestion by western blot analysis.

Incubation of IgG *ex vivo* in cynomolgus intestinal fluid followed by capture of mAb using an antiidiotype and detection by using an antibody against κ light chain region (thus detecting all fragments that include the Fab to full-length mAb) or the Fc region (to determine only

full-length mAb) showed that no full-length IgG1 was remaining by 60 min, whereas about 60% full-length IgG2 was retained in the same time period. This was confirmed by Commassie blue staining of the resulting fragments from IgG1 digestion that were consistent with Fc with core hinge fragments and two Fab fragments, which also indicates cleavage in the upper hinge region of the antibody. Engineered chimeric IgG1 with either a substitution of K222 to proline (data not shown) or a PVA substitution from IgG2 hinge, did not confer protease resistance. However, a chimeric IgG1 engineered with complete IgG2 hinge replacement showed molecular integrity similar to IgG2 by western blot. Consistent with these results, *in vivo* intestinal delivery of IgG2 resulted in 50% of anesthetized mice having intact mAb after 90 min, whereas IgG1 cleavage occurred in all cases. This time point was selected to be consistent with mouse small intestinal transit and the *in vitro* data showing that IgG1 proteolysis was mostly accomplished within 60 min. It should be noted that within 90 min incubation, IgG2 cleavage did occur in at least 50% of mice, suggesting that additional enzymes in some animals *in vivo* cleave IgG2, and that variable results might be expected in monkeys after intestinal delivery.

The IgG2 was engineered at position 428 as a M428L variant (Zalevsky *et al.* 2010) for improved FcRn binding affinity. Although we had previously confirmed cynomolgus FcRn binding using an antigrowth factor mAb, the binding affinity of the anti-RSV IgG2 M428L mAb was determined since factors involving a change in paratope can sometimes slightly alter FcRn binding, as well as to determine any effect of lyophilization, milling, and enteric coating. Cynomolgus FcRn binding of M428LIgG2 was assessed in head-to-head comparison of batch release (in pBS), lyophilized (in 10 mmol/L histidine, 8.5% sucrose, 0.04% PS80) milling, and also the contents after enteric-coated capsule dissolution (in FaSSIF) and indicated that the KD was consistently ~100 nmol/L. Therefore, binding to cynomolgus intestinal enterocyte FcRn, as well as endothelial cells to ensure longer circulating mAb half-life was confirmed at pH 6.0. Endosomal binding of mAb to FcRn at pH 6.0 prevents lysosomal degradation increasing its circulating serum half-life (Suzuki *et al.* 2010; Kuo and Aveson 2011). Thus, repeat dosing would be expected to result in systemic accumulation where the half-life is ~1 week. In the repeat dosing study, there was a doubling of the serum level after the second dose, but this apparent accumulation was not sustained by the second to third week of dosing and further increasing the dosing to biweekly, and then to two capsules/dose still did not achieve serum levels above 1 ng/mL. Since circulating half-life was calculated based on IV mAb dosed at

1 mg/kg, the clearance of mAb may not be linear (e.g., hysteresis) at the low levels circulating in this study.

Based on the results of numerous *in vitro* mechanistic studies in FcRn-expressing cells and *in vivo* functional studies in suckling neonates, many investigators have speculated that FcRn could be used as a means of mAb oral delivery. Therefore, we designed the FcRn validation and translation to primates to be as rigorous as possible to ensure that the functionality of the mAb was retained. The pH of the entire GI tract in cynomolgus was measured by state-of-the-art IntelliCap System[®] and reported here for the first time. Note that this finding is at variance with a recent comment regarding FcRn that gut pH had been measured only once, with litmus paper, and the observation was never repeated (Anderson 2014). The requirement was for the release of mAb in the small intestine where the pH was above pH 7.5 and thus where IgG will not bind to surface FcRn (Ward and Ober 2015). However, mAb released in the small intestine would rapidly enter the colon where the ~ pH 6 is due to microbiota production of short-chain fatty acids, and thus binding to enterocyte membrane surface FcRn might be expected (Cooper *et al.* 2014). Expression of FcRn was highest in the human colon (Hornby *et al.* 2014). Although high FcRn affinity IgG can accumulate within cells at neutral pH due to pinocytosis, and binding to FcRn in the endosomes, and is consistent with dynamic cycling of endosomal FcRn (Montoyo *et al.* 2009). Thus, our experimental design in cynomolgus should test the hypothesis that FcRn and fluid phase pinocytosis would be sufficient to allow IgG2 M428L entry into the enterocytes for trafficking and release on the systemic side.

Every effort was made to optimize the formulation to retain the biophysical properties and integrity of the mAb after formulation and lyophilization. In each case, these properties and the integrity of the full-length mAb were confirmed to be similar to the release batch dissolved in PBS. In addition, the cynomolgus intestinal pH profile enabled Eudragit[®] coating with the appropriate thickness for complete dissolution of the capsule in pH 7.5 and release of mAb within 5 min. Furthermore, because we were concerned about the pyloric sphincter ability to pass the capsule consistently, the initial testing was done *in vivo* after endoscopic delivery of capsules into the small intestine using a specially designed snare attached to the end of the endoscope. Subsequently, the six monkeys selected for oral dosing monkeys based on size 3 'dummy' capsules that were identically coated but filled with titanium oxide and confirmed by X-ray to passage out of the stomach.

The sensitive bioassay used and MSD method resulted in measurable levels of full-length mAb detected at most time points in the monkeys tested, with a PK profile that

was consistent with the dosing schedule and maximal levels obtained ~ 24 h after each dosing. However, this did not translate the *in vitro* evidence for FcRn-mediated mAb transcytosis (Dickinson *et al.* 1999; Claypool *et al.* 2002; Blumberg 2009). In contrast to endothelial cells, the FcRn–IgG complex is transferred through the intestinal epithelium cell and released on the basolateral side, and the disassociated IgG enters the lymphatic system and ultimately the circulation via the thoracic ducts (Swartz 2001; Kliwinski *et al.* 2013). The mechanism of uptake of IgG into the enterocytes remains quite controversial as to whether nonselective pinocytosis and cell-surface FcRn receptors both contribute to IgG internalization into the endosomes. In suckling rat pups, a contribution of membrane surface-expressed FcRn was demonstrated by using FcRn binding affinity variants and adjusting local intestinal pH (Cooper *et al.* 2014) but others have refuted any role of surface FcRn in the uptake of IgG by showing that IgG was present in intestinal enterocytes in mice lacking FcRn (Mohanty *et al.* 2013). Based on the low levels of mAb detected in systemic circulation in this study, it seems unlikely that active receptor-mediated internalization into enterocytes occurs to a meaningful extent. The absence of a dose-related uptake and apparent saturation despite increasing the dose or frequency of dosing, might be consistent with pinocytosis occurring at the luminal surface. If this speculation is correct then efforts to enhance FcRn binding would not increase further the uptake which depends on the efficiency of passive 'cell drinking'.

In non-human primates, bioavailability of an erythropoietin-Fc fusion protein was demonstrated after delivery to the upper and central airways, where FcRn epithelial expression in epithelial cells was highest (Bitonti *et al.* 2004). Indeed, in this study the monkey that accomplished the highest level (~6 ng/mL) serum mAb had bitten the capsule and may have inhaled the lyophilized mAb. The functionality of FcRn in the adult primate intestine may be less than the bronchiole epithelial FcRn, despite the fact that FcRn is visualized throughout the gastrointestinal tract in villous enterocytes (Israel *et al.* 1997; Shah *et al.* 2003).

In beagle dogs, IntelliCap[™] dosing of mAb in PBS did not result in detectable levels of mAb in serum despite the sensitivity of the assay. Human antibodies were cleared unusually quickly from the ferret presumably due to the lack of binding, whereas engineering a region of ferret FcRn can increase binding to human IgG (Nesspor and Scallan 2014). Aligning the canine FcRn public database sequence shows similarity to ferret FcRn suggesting that absence of human IgG binding to canine FcRn could account for the absence of serum levels. Furthermore, Madin–Darby canine kidney epithelial cells transfected to

express rat FcRn were used transcytosis/recycling experiments (Ramalingam et al. 2002) suggesting that endogenous canine FcRn lacks interactions with other IgGs.

Although the data point to the unfeasibility of using FcRn for oral bioavailability when delivered to small intestine and colon, we cannot completely rule out that proteolysis within an intestine resulted in loss of intact mAb prior to epithelial uptake since we did not develop the MSD mAb quantification assay for fecal material. Therefore, additional studies should be performed on whether IgG2 could be a local GI treatment where low systemic exposure is desirable. For example, an orally delivered bovine polyclonal anti-TNF, where enterocyte FcRn would not be expected to bind to bovine IgG, penetrated the colonic mucosa and inhibited TNF-driven mucosal inflammation with minimal systemic exposure in preclinical inflammatory models (Bhol et al. 2013).

Disclosure

All investigators are employees of Johnson & Johnson and have no other conflict of interest to disclose.

Acknowledgements

We thank Dr. William R. Strohl and Jill Giles-Komar (Janssen Biotherapeutics) for their support and enthusiasm for exploring the boundaries of bio-therapeutic delivery by validation of FcRn in translational models. We acknowledge the excellent evaluation of monkey and dog transit by Jeff Shimizu and Hans Zou (Medimetrics Briarcliff Manor, NY), and Lisa Laxson for technical assessment of mAb in FaSSiF. Valuable scientific discussions on formulation, chemico-physical evaluation and lyophilization involved Weiguo Dai, Bei Chen and Mark Chiu (Janssen Biotherapeutics) and on capsule and enteric coating by Dirk Roymans, Geert Verreck, Jurgen Mensch and David Breslin (Janssen Pharmaceutical Development Material Sciences).

References

Ageyama N, Shibata H, Narita H, Hanari K, Kohno A, Ono F, et al. (2001). Specific gravity of whole blood in cynomolgus monkeys (*Macaca fascicularis*), squirrel monkeys (*Saimiri sciureus*), and tamarins (*Saguinus labiatus*) and total blood volume in cynomolgus monkeys. *Contemp Top Lab Anim Sci* 40: 33–35.

Anderson CL (2014). There's been a flaw in our thinking. *Front Immunol* 5: 540.

Atha DH, Ingham KC (1981). Mechanism of precipitation of proteins by polyethylene glycols. Analysis in terms of excluded volume. *The Journal of biological chemistry* 256: 12108–12117.

Becker D, Zhang J, Heimbach T, Penland RC, Wanke C, Shimizu J, et al. (2014). Novel orally swallowable IntelliCap ((R)) device to quantify regional drug absorption in human GI tract using diltiazem as model drug. *AAPS PharmSciTech* 15: 1490–1497.

Benlounes N, Chedid R, Thuillier F, Desjeux JF, Rousselet F, Heyman M (1995). Intestinal transport and processing of immunoglobulin G in the neonatal and adult rat. *Biol Neonate* 67: 254–263.

Bhol KC, Tracey DE, Lemos BR, Lyng GD, Erlich EC, Keane DM, et al. (2013). AVX-470: a novel oral anti-TNF antibody with therapeutic potential in inflammatory bowel disease. *Inflamm Bowel Dis* 19: 2273–2281.

Bitonti AJ, Dumont JA, Low SC, Peters RT, Kropp KE, Palombella VJ, et al. (2004). Pulmonary delivery of an erythropoietin Fc fusion protein in non-human primates through an immunoglobulin transport pathway. *Proc Natl Acad Sci USA* 101: 9763–9768.

Blumberg RS, Lencer WL, Simister NE, (2009) Receptor specific transepithelial transport of therapeutics. US Patent Office 754736:1–26.

Claypool SM, Dickinson BL, Yoshida M, Lencer WI, Blumberg RS (2002). Functional reconstitution of human FcRn in Madin-Darby canine kidney cells requires co-expressed human beta 2-microglobulin. *J Biol Chem* 277: 28038–28050.

Claypool SM, Dickinson BL, Wagner JS, Johansen FE, Venu N, Borawski JA, et al. (2004). Bidirectional transepithelial IgG transport by a strongly polarized basolateral membrane Fcγ-receptor. *Mol Biol Cell* 15: 1746–1759.

Cooper PR, Kliwinski CM, Perkinson RA, Ragwan E, Mabus JR, Powers GD, et al. (2014). The contribution of cell surface FcRn in monoclonal antibody serum uptake from the intestine in suckling rat pups. *Front. Pharmacol.* 5: 225.

de la Cruz Perez Moreno M., Oth M, Deferme S, Lammert F, Tack J, Dressman J, et al. (2006). Characterization of fasted-state human intestinal fluids collected from duodenum and jejunum. *J. Phar. Pharmacol.* 58: 1079–1089.

Dickinson BL, Badizadegan K, Wu Z, Ahouse JC, Zhu X, Simister NE, et al. (1999). Bidirectional FcRn-dependent IgG transport in a polarized human intestinal epithelial cell line. *J. Clin. Investig.* 104: 903–911.

Evans DF, Pye G, Bramley R, Clark AG, Dyson TJ, Hardcastle JD (1988). Measurement of gastrointestinal pH profiles in normal ambulant human subjects. *Gut* 29: 1035–1041.

He W, Ladinsky MS, Huey-Tubman KE, Jensen GJ, McIntosh JR, Bjorkman PJ (2008). FcRn-mediated antibody transport across epithelial cells revealed by electron tomography. *Nature* 455: 542–546.

Hornby PJ, Cooper PR, Kliwinski C, Ragwan E, Mabus JR, Harman B, et al. (2014). Human and Non-Human Primate

Intestinal FcRn Expression and Immunoglobulin G Transcytosis. *Pharm Res* 31: 908–922.

Israel EJ, Taylor S, Wu Z, Mizoguchi E, Blumberg RS, Bhan A, et al. (1997). Expression of the neonatal Fc receptor, FcRn, on human intestinal epithelial cells. *Immunology* 92: 69–74.

Kliwinski C, Cooper PR, Perkinson R, Mabus JR, Tam SH, Wilkinson TM, et al. (2013). Contribution of FcRn binding to intestinal uptake of IgG in suckling rat pups and human FcRn-transgenic mice. *Am J Physiol Gastrointest Liver Physiol* 304: G262–G270.

Kuo TT, Aveson VG (2011). Neonatal Fc receptor and IgG-based therapeutics. *MABS* 3: 422–430.

Low SC, Nunes SL, Bitonti AJ, Dumont JA (2005). Oral and pulmonary delivery of FSH-Fc fusion proteins via neonatal Fc receptor-mediated transcytosis. *Hum Reprod* 20: 1805–1813.

Mabus JR, Muzammil S, Cooper PR, Brezski R, Kunta J, Huebert ND, et al. (2014) Enteric-coated capsule intestinal delivery of human IgG in cynomolgus macaques. *FASEB J*. 28 (Supplement 1):LB603.

Martin MG, Wu SV, Walsh JH (1997). Ontogenetic development and distribution of antibody transport and Fc receptor mRNA expression in rat intestine. *Dig Dis Sci* 42: 1062–1069.

Maurer JM, Schellekens RC, van Rieke HM, Wanke C, Iordanov V, Stellaard F, et al. (2015). Gastrointestinal pH and Transit Time Profiling in Healthy Volunteers Using the IntelliCap System Confirms Ileo-Colonic Release of ColoPulse Tablets. *PLoS ONE* 10: e0129076.

Medgyesi GA, Csécsi-Nagy M, Gorini G, Puskas E, Gergely J, Sajgo M, et al. (1973). Fab-related fragments of human IgG produced by partial tryptic proteolysis. *Immunochemistry* 10: 509–515.

Mohanty S, Kim J, Ganesan LP, Phillips GS, Robinson JM, Anderson CL (2013). Abundant Intracellular IgG in Enterocytes and Endoderm Lacking FcRn. *PLoS ONE* 8: e70863.

Montoyo HP, Vaccaro C, Hafner M, Ober RJ, Mueller W, Ward ES (2009). Conditional deletion of the MHC class I-related receptor FcRn reveals the sites of IgG homeostasis in mice. *Proc Natl Acad Sci USA* 106: 2788–2793.

Nesspor TC, Scallon B (2014). Chimeric antibodies with extended half-life in ferrets. *Influenza Other Respir Viruses* 8: 596–604.

Petkova SB, Akilesh S, Sproule TJ, Christianson GJ, Al Khabbaz H, Brown AC, et al. (2006). Enhanced half-life of genetically engineered human IgG1 antibodies in a humanized FcRn mouse model: potential application in humorally mediated autoimmune disease. *Int Immunol* 18: 1759–1769.

Pridgen EM, Alexis F, Kuo TT, Levy-Nissenbaum E, Karnik R, Blumberg RS, et al. (2013). Transepithelial transport of fc-targeted nanoparticles by the neonatal fc receptor for oral delivery. *Sci Transl Med* 5:213ra167.

Ramalingam TS, Detmer SA, Martin WL, Bjorkman PJ (2002). IgG transcytosis and recycling by FcRn expressed in MDCK cells reveals ligand-induced redistribution. *EMBO J* 21: 590–601.

Shah U, Dickinson BL, Blumberg RS, Simister NE, Lencer WI, Walker WA (2003). Distribution of the IgG Fc receptor, FcRn, in the human fetal intestine. *Pediatr Res* 53: 295–301.

Shields RL, Namenuk AK, Hong K, Meng YG, Rae J, Briggs J, et al. (2001). High resolution mapping of the binding site on human IgG1 for Fc gamma RI, Fc gamma RII, Fc gamma RIII, and FcRn and design of IgG1 variants with improved binding to the Fc gamma R. *J Biol Chem* 276: 6591–6604.

Steidler L, Hans W, Schotte L, Neiryneck S, Obermeier F, Falk W, et al. (2000). Treatment of murine colitis by *Lactococcus lactis* secreting interleukin-10. *Science* 289: 1352–1355.

Suzuki T, Ishii-Watabe A, Tada M, Kobayashi T, Kanayasu-Toyoda T, Kawanishi T, et al. (2010). Importance of neonatal FcR in regulating the serum half-life of therapeutic proteins containing the Fc domain of human IgG1: a comparative study of the affinity of monoclonal antibodies and Fc-fusion proteins to human neonatal FcR. *J Immunol*. 184: 1968–1976.

Swartz MA (2001). The physiology of the lymphatic system. *Adv Drug Deliv Rev* 50: 3–20.

Uno Y, Utoh M, Iwasaki K (2014). Polymorphisms of neonatal Fc receptor in cynomolgus and rhesus macaques. *Drug Metab Pharmacokinet* 29: 427–430.

Vandenbroucke K, de Haard H, Beirnaert E, Dreier T, Lauwereys M, Huyck L, et al. (2010). Orally administered *L. lactis* secreting an anti-TNF Nanobody demonstrate efficacy in chronic colitis. *Mucosal Immunol* 3: 49–56.

Ward ES, Ober RJ (2015). Commentary: “There’s been a flaw in our thinking”. *Front Immunol* 6: 351.

Zalevsky J, Chamberlain AK, Horton HM, Karki S, Leung IW, Sproule TJ, et al. (2010). Enhanced antibody half-life improves in vivo activity. *Nat Biotechnol* 28: 157–159.